Reversing the direction of the supercurrent in a controllable Josephson junction

Baselmans, J.J.A.; Morpurgo, A.F.; Wees, B.J. van; Klapwijk, T.M.

Published in:
Nature

Publication date:
1999

Received 23 September; accepted 20 October 1998.

1. Hurley, K. in *Proc. 3rd Huntsville Symp.* (eds Kouveliotou, C., Briggs, M. and Fishman, G.) 889–896 (AIP Conf. Proc. 384, Am. Inst. Phys., New York, 1996).
2. Mazets, E., Golenetskii, S., Guryan, Yu. & Ilyinskii, V. The 5 March 1979 event and the distinct class of short gamma bursts: are they of the same origin? *Astrophys. Space Sci.* **84,** 173–189 (1982).
3. Barat, C. *et al.* Evidence for periodicity in a gamma ray burst. *Astron. Astrophys.* **79,** L24–L25 (1979).
4. Braun, R., Goss, W. & Lyne, A. Three fields containing young pulsars: the observable lifetime of supernova remnants. *Astrophys. J.* **340,** 355–361 (1989).
5. Thompson, C. & Duncan, R. The soft gamma repeaters as very strongly magnetized neutron stars. I. Radiative mechanism for outbursts. *Mon. Not. R. Astron. Soc.* **275,** 255–300 (1995).
6. Mazets, E. *et al.* A flaring X-ray pulsar in Dorado. *Nature* **282,** 587–589 (1979).
7. Cline, T. *et al.* Detection of a fast, intense and unusual gamma ray transient. *Astrophys. J.* **237,** L1–L5 (1980).
8. Golenetskii, S., Ilinskii, V., Mazets, E. & Guryan, Yu. Repeating gamma ray bursts from the source FXP 0520-66. *Sov. Astron. Lett.* **5,** 340–342 (1979).
9. Golenetskii, S., Ilyinskii, V. & Mazets, E. Recurrent bursts in the source of the 5 March 1979 event. *Nature* **307,** 41–43 (1984).
10. Evans, W. *et al.* Location of the gamma-ray transient event of 1979 March 5. *Astrophys. J.* **237,** L7–L9 (1980).
11. Cline, T. *et al.* Precise source location of the anomalous 1979 March 5 gamma ray transient. *Astrophys. J.* **255,** L45–L48 (1982).
12. Rothschild, R., Kulkarni, S. & Lingenfelter, R. Discovery of an X-ray source coincident with the soft gamma repeater 0525-66. *Nature* **368,** 432–434 (1994).
13. Mazets, E., Golenetskii, S. & Guryan, Yu Soft gamma ray bursts from the source B1900+14. *Sov. Astron. Lett.* **5(6)** 343–344 (1979).
14. Kouveliotou, C. *et al.* Recurrent burst activity from the soft gamma-ray repeater SGR 1900+14. *Nature* **362,** 728–730 (1993).
15. Kouveliotou, C. *et al.* The rarity of soft gamma-ray repeaters deduced from reactivation of SGR1806-20. *Nature* **368,** 125–127 (1994).
16. Vasisht, G., Kulkarni, S., Frail, D. & Greiner, J. Supernova remnant candidates for the soft gamma-ray repeater 1900+14. *Astrophys. J.* **431,** L35–L38 (1994).
17. Hurley, K. *et al.* Network synthesis localization of two soft gamma repeaters. *Astrophys. J.* **431,** L31–L34 (1994).
18. Hurley, K., Kouveliotou, C., Mazets, E. & Cline, T. *IAU Circ.* No. 6929 (1998).
19. Hurley, K. *et al.* Reactivation and precise IPN localization of the soft gamma repeater SGR1900+14. *Astrophys. J.* (in the press).
20. Hurley, K., Cline, T., Mazets, E. & Golenetskii, S. *IAU Circ.* No. 7004 (1998).
21. Hurley, K., Kouveliotou, C., Murakami, T. & Strohmayer, T. *IAU Circ.* No. 7001 (1998).
22. Kouveliotou, C., Strohmayer, T., Hurley, K., van Paradijs, J. & Woods, P. *IAU Circ.* No. 7001 (1998).
23. Cline, T., Mazets, E. & Golenetskii, S. *IAU Circ.* No. 7002 (1998).
24. Marshall, F. *et al. IAU Circ.* No. 7005. (1998).
25. Kouveliotou, C. *et al.* An X-ray pulsar with a superstrong magnetic field in the soft gamma-ray repeater SGR1806-20. *Nature* **393,** 235–237 (1998).
26. Barat, C. *et al.* Fine time structure in the 1979 March 5 gamma-ray burst. *Astron. Astrophys.* **126,** 400–402 (1983).
27. Fenimore, E., Klebesadel, R. & Laros, J. The 1979 March 5 gamma-ray transient: was it a classical gamma-ray burst? *Astrophys. J.* **460,** 964–975 (1996).
28. Hurley, K. *et al.* The solar X-ray/cosmic gamma-ray burst experiment abroad Ulysses. *Astron. Astrophys. Suppl. Ser.* **92,** 401–410 (1992).

Acknowledgements. We thank R. Duncan for discussions about the magnetic field estimate. This work was supported in the US by NASA and a contract from JPL, and at the Ioffe Institute by an RSA contract.

Correspondence and requests for materials should be addressed to K.H. (e-mail: khurley@sunspot.ssl.verkeleg.edu).

Reversing the direction of the supercurrent in a controllable Josephson junction

J. J. A. Baselmans*, A. F. Morpurgo*†, B. J. van Wees* & T. M. Klapwijk*

** Department of Applied Physics and Material Science Center, University of Groningen, Nijenborgh 4, 9747 AG Groningen, The Netherlands*

When two superconductors are connected by a weak link, a supercurrent flows, the magnitude of which is determined by the difference in the macroscopic quantum phases of the superconductors. This phenomenon was discovered by Josephson[1] for the case of a weak link formed by a thin tunnel barrier: the supercurrent, *I*, is related to the phase difference, ϕ, through the Josephson current–phase relation, $I = I_c \sin\phi$, with I_c being the critical current which depends on the properties of the weak link. A similar relation holds for weak links consisting of a normal metal, a semiconductor or a constriction[2]. In all cases, the phase difference is zero when no supercurrent flows through the junction, and increases monotonically with increasing supercurrent until the critical current is reached. Here we use nanolithography techniques to fabricate a Josephson junction with a normal-metal weak link in which we have direct access to the microscopic current-carrying electronic states inside the link. We find that the fundamental Josephson relation can be changed from $I = I_c \sin\phi$ to $I = I_c \sin(\phi + \pi)$—that is, a π-junction—by controlling the energy distribution of the current-carrying states in the normal metal. This fundamental change in the way these Josephson junctions behave has potential implications for their use in superconducting electronics as well as in (quantum) logic circuits based on superconductors.

The microscopic mechanism responsible for the supercurrent in a Josephson junction is the transport of correlated electrons. In a superconductor/normal-metal/superconductor (SNS) junction, conduction electrons mediate current transport from superconductor 1 (S1) to superconductor 2 (S2) by either ballistic or diffusive transport through the normal metal (N). In a ballistic junction, in which the elastic mean free path is larger than the length of the normal region, Andreev bound states are formed[3–5]. The dispersion relation of these states is such that each subsequent state carries a supercurrent in the positive or negative direction at a given value of the macroscopic phase difference between the superconductors; the states are degenerate if the phase is zero. The net supercurrent that flows between the two superconductors depends therefore not only on the actual phase difference ϕ, but also on the occupation of the Andreev bound states. The prediction is that the electron energy distribution function in the normal region will change the supercurrent, even resulting in a sign reversal[6–8].

Transport of electrons in metals is usually diffusive, the electron trajectories are not well defined, and Andreev bound states are no longer the natural concept to describe the supercurrent. But electron correlations induced by the superconducting electrodes are still present, with the energy scale determined by the Thouless energy $E_T = \hbar D/L^2$, where D is the diffusion coefficient and L is the separation between the superconductors. The energy spectrum of the superconducting correlations is expressed in a so-called supercurrent-carrying density of states, which can be calculated directly using the quasiclassical Green's function theory of superconductivity[9–12]. The supercurrent-carrying density of states is an odd function of energy; it shows a phase-dependent mini-gap at low energies, above which it has a positive maximum, after which it changes sign and approaches zero at high energies. The positive and negative

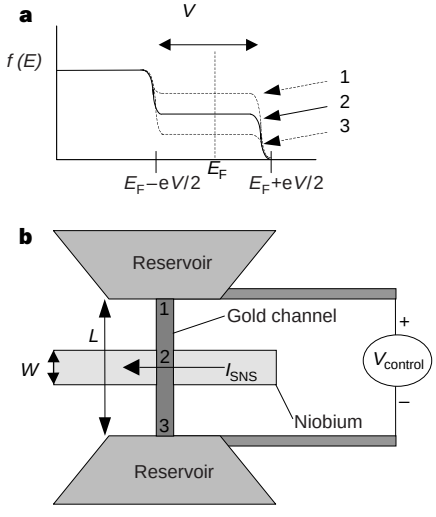

Figure 1 Electronic distribution function and the sample layout. In the bottom panel, a gold channel between two electron reservoirs is connected to two niobium superconducting leads. The control voltage across the channel induces a position-dependent electron distribution, shown in **a** for positions 1, 2 and 3 in **b**. The current through the Josephson junction is indicated by I_{SNS}.

† Present address: Department of Physics, Stanford University, Stanford, California 94305-4060, USA.

parts of the supercurrent-carrying density of states represent, at a given phase, energy-dependent contributions to the supercurrent in the positive and negative direction. The size and direction of the total supercurrent depends therefore on the occupied fraction of these states, which is analogous to the occupation of the discrete Andreev bound states in a ballistic system. In a recent experiment, Morpurgo *et al.*[13] changed the occupied fraction of the supercurrent-carrying density of states by raising the effective electron temperature. This was done by sending a normal current from normal reservoirs through the N-part of the SNS junction, leading to a Fermi–Dirac distribution with the electrons at a slightly elevated temperature. A monotonic decrease of the supercurrent was observed, which is expected for a thermal distribution.

In a mesoscopic wire, however, the distribution of electrons over the energies is not necessarily thermal. As shown by Pothier *et al.*[14,15], the electron distribution in a normal wire attached to two large electron reservoirs at a voltage difference V may have a double-step structure. A non-equilibrium state is reached by changing the chemical potentials of the electron reservoirs in opposite directions by applying a control voltage. The energy of the electrons in the wire depends on the distribution functions of the reservoirs, possibly modified by inelastic relaxation processes inside the wire. If the wire is sufficiently short, so that the diffusion time τ_D is smaller than the inelastic scattering time τ_i, the energy of the electrons will be conserved over the length of the wire. The energy distribution of the electrons in the channel is then given by the superposition of the Fermi–Dirac distributions of the reservoirs. This results, at sufficiently low temperatures $k_BT \ll eV$ (where k_B is Boltzmann's constant and e the single electron charge), in a position-dependent double-step function (Fig. 1a). The energy separation between the steps is eV. As predicted[9–12], such an energy distribution will have a profound effect on the supercurrent in an SNS junction, even reversing its direction for sufficiently large control voltages. The microscopic mechanism responsible for this is the redistribution of the occupied fraction of the current-carrying density of states due to the change in the electronic distribution function inside the junction. The stable zero-current state, which corresponds to $\phi = 0$ for a conventional Josephson junction, corresponds to $\phi = \pi$ at large control voltages, resulting in a current–phase relation given by $I = I_c\sin(\phi + \pi)$, hence the name π-junction. This mechanism should not be confused with the π-junction behaviour induced by magnetic impurities (refs 16, 17 and references therein) or resulting from the symmetry of the order parameter in ceramic superconductors (ref. 18 and references therein). Not only are the microscopic mechanisms different in these cases, but in our case the junction is also controllable, its state depending on the applied control voltage.

We study the behaviour of the Josephson current in four similar diffusive SNS junctions by applying a non-thermal distribution function to the normal conducting weak link. We present the results of one device. The device is shown in Fig. 1b. A thin (~40 nm) and narrow (~200 nm) gold channel is connected to two relatively thick (475 nm) electron reservoirs of millimetre size. In the other direction, the gold channel is coupled in its centre to two superconducting niobium electrodes. The distance between the two niobium electrodes is 300 nm. The measurements are performed at 100 mK to realize a sharp Fermi–Dirac distribution function inside the reservoirs. Electronic filtering at room temperature and at 100 mK is used to reduce external noise and hence, unintentional heating of the electrons. The gold of the channel has a diffusion coefficient at 180 $cm^2\,s^{-1}$, resulting in a Thouless energy $E_T \approx 140\,\mu eV$, so that at the measuring temperature $k_BT = 10\,\mu eV < E_T < \Delta = 1{,}500\,\mu eV$ (here Δ is the superconducting energy gap of niobium). The length of the control channel between the reservoirs, L, is 1 μm, resulting in an estimated diffusion time of $\tau_D = 50$ ps. This is much smaller than the estimated energy relaxation time for electrons in a thin film of impure gold[19]. The reservoirs are of millimetre size because they also need to act as effective cooling fins to prevent unwanted electron heating and hence maintain the desired step-like electron distribution[20]. The contacts between the gold and the niobium are cleaned using argon sputter etching to ensure a high interface transparency.

In the experiment, the current–voltage (I–V) curves of the SNS junction are measured for different values of control voltage across the control channel ($V_{control}$). From these curves, we determine the critical current of the junction as a function of the control voltage (Fig. 2). The critical current of the SNS junction shows a non-monotonic behaviour as a function of control voltage. At zero control voltage, the product I_cR_n (where R_n is the normal state resistance of the junction), 200 μV, is of the order of the Thouless energy, in good agreement with the theory of diffusive SNS junctions[21]. When a voltage is applied, the distribution function

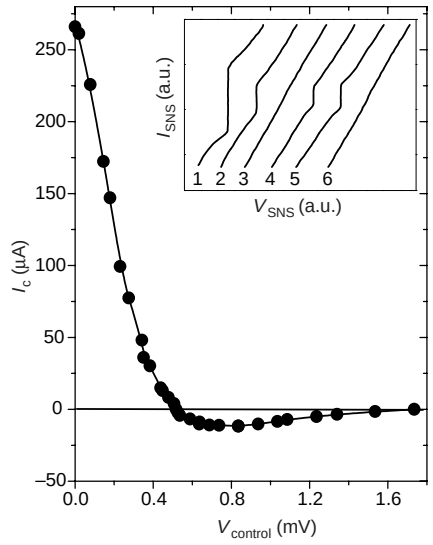

Figure 2 Critical current of the SNS junction as a function of the control voltage. The current is plotted negative above $V_{critical} = 0.52$ meV because of the π-state of the junction; a.u., arbitrary units. Inset, selected I–V curves for the following control voltages: 0.38 mV (curve 1), 0.44 mV (2), 0.52 mV (3), 0.64 mV (4), 0.84 mV (5), 1.70 mV (6).

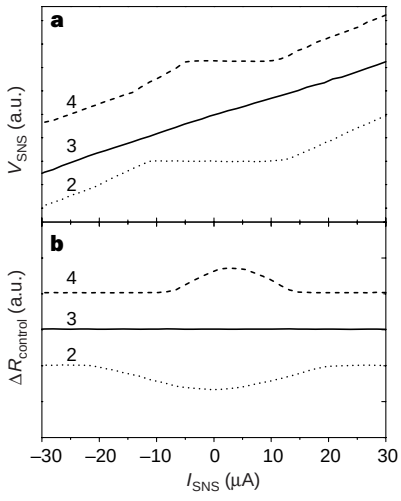

Figure 3 V_{SNS}, the voltage across the junction, and the resistance of the control channel as a function of the current I_{SNS} for three different values of the control voltage. The curves in **a** and **b** correspond to curves 2, 3 and 4 of Fig. 2 inset (offset for clarity). The resistance variation changes sign, although the corresponding I–V curves look similar for $V_{control} < V_{critical}$ (2) or $V_{control} < V_{critical}$ (4).

inside the gold wire changes, and therefore the occupation of the energy levels carrying the supercurrent also changes. A decrease of the supercurrent is observed, reaching zero at $V_{control} = 520\,\mu V \equiv V_{critical}$, corresponding to approximately four times the Thouless energy; no sign of a supercurrent can be detected (Fig. 2, inset). At higher voltages, the supercurrent reappears. In Fig. 2 we plot the critical supercurrent in this region with a minus sign, anticipating that the junction has entered the π-state. Above voltages of 1.7 meV, no supercurrent can be detected.

To determine the current–phase relation, $I = I_c \sin(\phi)$ or $I = I_c \sin(\phi + \pi)$, we need an independent way to determine the phase difference across the junction for a fixed direction of the applied supercurrent. We recall that the normal conductance of the control channel is also modulated by the phase difference ϕ—a phenomenon known as Andreev interferometry and extensively studied in recent years[22,23]. The modulation of the conductance arises from the fact that Andreev reflected holes scatter from both superconductors with a different phase shift, and therefore might interfere constructively ($\phi = 0$) or destructively ($\phi = \pi$). This leads to a phase-dependent change in the diffusion constant in N. The resulting phase dependence of the resistance is given approximately by $\Delta R = -R_0(1 + \cos(\phi))$, where R_0 has a temperature- and energy-dependent amplitude.

In Fig. 3 we show the resistance of the normal control channel (Fig. 3b) and the observed I–V curves of the SNS junction (Fig. 3a). The dependence of ΔR on the applied current changes sign on crossing the critical control voltage. The middle curve (3) shows no modulation at all; the corresponding I–V curve is linear. If we suppose that the current–phase relation is given by the conventional Josephson relation $I = I_c \sin(\phi)$, then the phase difference between the two superconductors changes from $-\pi/2$ through 0 to $\pi/2$ if the current through the junction I_{SNS} is varied from $-I_c$ to $+I_c$. Hence the resistance of the control channel will show a minimum at $I_{SNS} = 0$, corresponding to $\phi = 0$. This is observed for all control voltages $V_{control} < V_{critical}$. The upper curve in Fig. 3b is an example of the behaviour for $V_{control} > V_{critical}$: a maximum is observed in the resistance for $I_{SNS} = 0$, consistent with the assumption that the current–phase relation is now given by $I = I_c \sin(\phi + \pi)$ and $\phi = \pi$ when $I_{SNS} = 0$. The phase difference π between the two superconductors appears whenever $V_{control} > V_{critical}$. We take this as direct proof that the junction switches from a normal state to a π-state as a function of the control voltage.

The qualitative dependence of I_c on $V_{control}$, and the energy at which the phase jumps, are both in agreement with theoretical work on diffusive SNS junctions[10–12]. However, the relative magnitude of the supercurrent in the π-state range of $V_{control}$ is smaller than one would expect in comparison to I_c at $V_{control} = 0$. The most important reason for this is probably the geometry of the sample. In our case, the width-to-length ratio W/L is ~0.4, so that the distribution function is not constant over the entire junction length. This will reduce the magnitude of the supercurrent in the π-regime, as predicted theoretically[9]. □

Received 9 July; accepted 30 September 1998.

1. Josephson, B. D. Possible new effects in superconducting tunneling. *Phys. Lett.* **1,** 251–253 (1962).
2. Likharev, K. K. Superconducting weak links. *Rev. Mod. Phys.* **51,** 101–169 (1979).
3. Kulik, I. O. Macroscopic quantization and the proximity effect in S-N-S junctions. *Zh. Eksp. Teor. Fiz.* **57,** 1745–1750 (1969); *Sov. Phys. JETP* **30,** 944–950 (1970).
4. Ishii, C. Josephson currents through junctions with normal metal barriers. *Prog. Theor. Phys.* **5,** 1525–1547 (1972).
5. Bardeen, J. & Johnson, J. L. Josephson current flow in pure superconducting-normal-superconducting junctions. *Phys. Rev. B* **5,** 72–78 (1972).
6. Van Wees, B. J., Lenssen, K.-M. H. & Harmans, C. J. P. M. Transmission formalism for supercurrent flow in multiprobe superconductor-semiconductor devices. *Phys. Rev. B* **44,** 470–473 (1991).
7. Wendin, G. & Shumeiko, V. S. Giant Josephson current through a single bound state in a superconducting tunnel junction. *Phys. Rev. B* **53,** R6006–R6009 (1996).
8. Chang, L.-F. & Bagwell, P. F. Control of Andreev level occupation in a Josephson junction by a normal metal probe. *Phys. Rev. B* **55,** 12678–12690 (1997).
9. Volkov, A. F. New phenomena in Josephson SINIS junctions. *Phys. Rev. Lett.* **74,** 4730–4733 (1995).
10. Volkov, A. F. & Takayamagi, H. Long range phase coherent effects in the transport properties of mesoscopic superconductor–normal-metal structures. *Phys. Rev. B* **56,** 11184–11194 (1997).
11. Wilhelm, F. K., Schön, G. & Zaikin, A. D. Mesoscopic superconducting-normal metal-superconducting transistor. *Phys. Rev. Lett.* **81,** 1682–1685 (1998).
12. Yip, S.-K. Energy resolved supercurrent between two superconductors. *Phys. Rev. B* **58,** 5803–5807 (1998).
13. Morpurgo, A. F., Klapwijk, T. M. & van Wees, B. J. Hot electron tunable supercurrent. *Appl. Phys. Lett.* **72,** 966–968 (1998).
14. Pothier, H., Guéron, S., Birge, N. O., Esteve, D. & Devoret, M. H. Energy distribution function of quasiparticles in mesoscopic wires. *Phys. Rev. Lett.* **79,** 3490–3493 (1997).
15. Pothier, H., Guéron, S., Birge, N. O., Estève, D. & Devoret, M. H. Energy distribution of electrons in an out-of-equilbrium metallic wire. *Z. Phys. B* **104,** 178–182 (1997).
16. Bulaevski, L. N., Kuzii, V. V. & Sobyanin, A. A. On possibility of spontaneous magnetic flux in a josephson junction containing magnetic impurities. *Solid State Commun.* **25,** 1053–1057 (1978).
17. Mühge, Th. *et al.* Possible origin for oscillatory superconducting transition temperature in superconducting/ferromagnet multilayers. *Phys. Rev. Lett.* **77,** 1857–1860 (1996).
18. van Harlingen, D. J. Phase-sensitive tests of the symmetry of the pairing state in high-temperature superconductors—evidence for $d_{x^2-y^2}$ symmetry. *Rev. Mod. Phys.* **67,** 515–535 (1995).
19. Echternach, P. M., Ghershenson, M. E. & Bozler, M. H. Evidence of interference between electron-phonon and electron-impurity scattering on the conductivity of thin metal films. *Phys. Rev. B* **47,** 13659–13663 (1993).
20. Wellstood, F. C., Urbina, C. & Clarke, J. Hot electron effects in metals. *Phys. Rev. B* **49,** 5942–5955 (1994).
21. Wilhelm, F. K., Zaikin, A. D. & Schön, G. Supercurrent in a mesoscopic proximity wire. *J. Low Temp. Phys.* **106,** 305–310 (1997).
22. Estève, D. *et al.* in *Mesoscopic Electron Transport: NATO ASI series E*, vol. 345 375–406 (eds Sohn, L. L. *et al.*) (Kluwer Academic, Dordrecht/Boston/London, 1997).
23. Van Wees, B. J. & Takayanagi, H. in *Mesoscopic Electron Transport: NATO ASI series E*, vol. 345, 469–502 (eds Sohn, L. L. *et al.*) (Kluwer Academic, Dordrecht/Boston/London, 1997).

Acknowledgements. We thank F. K. Wilhelm for discussions. This work was supported by the Nederlandse Organisatie voor Wetenschappelijk Onderzoek (NWO) through the Stichting voor Fundamenteel Onderzoek der Materie (FOM).

Correspondence and requests for materials should be addressed to J.J.A.B. (e-mail: Baselman@phys.rug.nl).

Scaling of transition temperature and CuO_2 plane buckling in a high-temperature superconductor

O. Chmaissem*†, J. D. Jorgensen†, S. Short†, A. Knizhnik‡, Y. Eckstein‡ & H. Shaked§

** Science and Technology Center for Superconductivity, and † Materials Science Division, Argonne National Laboratory, Argonne, Illinois 60439, USA*
‡ Department of Physics and Crown Center for Superconductivity, Technion, Haifa 32000, Israel
§ Department of Physics, Ben Gurion University, Beer-Sheva 84105, Israel

A characteristic feature of the high-temperature superconductors is the existence of a chemical composition that gives a maximum transition temperature, T_c, separating the so-called under-doped and over-doped regimes[1,2]. This behaviour is thought to be universal for high-temperature superconductors. In practice, there are only a few high-T_c compounds for which the composition can be varied continuously throughout the entire doping range. Here we report a study of correlations between structure and T_c in a compound with the '123' structure in which both the under-doped and over-doped regimes can be accessed. We observe a clear scaling between T_c and the buckling of the copper oxide planes; both go through a maximum at the same oxygen composition (and hence doping level), so implying a common origin. Previous work has shown that, for a fixed chemical composition, increased CuO_2 plane buckling lowers the transition temperature[3–11]. Thus the observation of a maximum in the buckling at the maximum T_c indicates that, as the composition is changed to increase T_c, there is a structural response that competes with superconductivity.

The 123 compound used for these studies is $(La_{1-x}Ca_x)(Ba_{1.75-x}La_{0.25+x})Cu_3O_y$ (ref. 12). In previous work[12], it has been shown that this compound can be readily made as a single phase, with the cation substitutions as indicated by the formula, for $0 \leqslant x \leqslant 0.4$. Powder samples of $(La_{1-x}Ca_x)(Ba_{1.75-x}La_{0.25+x})Cu_3O_y$ with $x = 0.1$ and 0.4 were synthesized by the methods described previously[12]. The